Impurity-Related Linear and Nonlinear Optical Absorption Coefficients of Unstrained (In,Ga)N-GaN Symmetric Coupled QWs

H. El Ghazi[a,b,*] and A. John Peter[c]

[a]LPS, Faculty of Science, Dhar EL Mehrez, BP 1796 Fes-Atlas, Morocco

[b]Special Mathematics, CPGE Rabat, Morocco

[c]Department of Physics, Govt. Arts and Science College, Melur-625106, Madurai, India

(Received April 29, 2014; in final form December 6, 2014)

Linear, third-order nonlinear and total optical absorption coefficients associated with intra-conduction band in wurtzite unstrained (In,Ga)N-GaN coupled quantum wells are calculated. Based on the effective-mass and the one-band parabolic approximations, the well and the barrier-widths effects are investigated variationally under finite confinement potential barrier. The results indicate that the structure size have a great influence on the optical properties. The results reveal also that larger optical absorption coefficients are obtained compared to single quantum well and a significant red-shift is obtained as the structure size increases. It is found that the modulation of the absorption coefficients can be easily obtained by adjusting the barrier and/or the well widths.

DOI: 10.12693/APhysPolA.127.787

PACS: 78.67.De, 78.20.Ci, 42.65.–k

1. Introduction

The discovery of the narrow band-gap energy of InN at 0.78 eV opened up many new ways for III-nitrides applications. It has been recognized that the band-gap energy of InGaN ternary alloy system can vary from 0.78 to 3.42 eV which covers almost the entire solar spectrum. In conjunction with other advantages of a direct band-gap, great radiation resistance, chemical and thermal stabilities and high absorption coefficient (10^4 cm^{-1}) make it as an excellent candidate for high-power, high-temperature electronic devices, such as high-brightness blue-green light emitting diodes (LEDs), laser diodes (LDs), infrared photo detectors, far-infrared laser amplifiers, optical memory technology, high-speed electro-optical modulators and so on. The nonlinear optical properties of single quantum well have been studied systematically [1–7]. Symmetric and asymmetric coupled quantum systems have attracted much interest both theoretically and experimentally. For instance, Zhang et al. [8] have reported the second-harmonic generation susceptibility in wurtzite nitride double quantum wells (QWs). Bedoya and Camacho [9] investigate the effect of the external electric field on the linear and nonlinear intersubband optical absorption coefficients (OACs) in asymmetric coupled QW. Additionally, Park et al. [10] reported the theoretical study of the second-order nonlinear optical susceptibility in asymmetric undoped (Al,Ga)As-(In,Ga)As double QWs. Ozturk and Sokmen [11] theoretically calculate the intersubband optical absorption in an asymmetric double quantum well for different barrier widths and the right well widths. Chen et al. [12] study the second harmonic generation in the asymmetric coupled quantum wells (ACQWs) theoretically for different widths of the right-well and the barrier. Recently, the optical properties of the asymmetric double semiparabolic quantum wells are investigated numerically for typical GaAs/Al$_x$Ga$_{1-x}$As [13]. To the best of our knowledge, no work has been done to treat the structure size effect on optical properties of (In,Ga)N-GaN coupled QWs.

In this paper, we will attempt to investigate the coupling effects on the OACs associated with intra-conduction band transition in wurtzite unstrained (In,Ga)N-GaN symmetric coupled QWs (SCQW).

2. Theoretical framework

We consider a wurtzite (In,Ga)N-GaN unstrained symmetric coupled quantum wells (SCQW) structure. The schematic description of the structure and the corresponding confinement potential are shown in Fig. 1. The reference of the structure is taken at the center of the middle barrier region.

Within the framework of the effective-mass and single band parabolic approximations, the Hamiltonian of an on-center shallow donor impurity in wurtzite (In,Ga)N-GaN unstrained DCQW can be expressed as follows:

$$H = -\frac{\hbar^2}{2m*}\Delta - \frac{e^2}{\varepsilon^* r} + V(z). \tag{1}$$

e is the electron charge and $r(=\sqrt{x^2+y^2+z^2})$ is the e–impurity distance. ε^* and m^* are, respectively, the main relative dielectric constant and the effective-mass. $V(z)$ is the growth-direction confinement potential given as

*corresponding author; e-mail: hadghazi@gmail.com

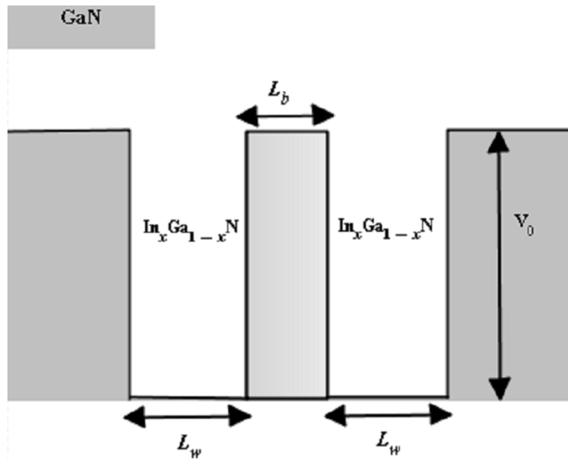

Fig. 1. The schematic description of the unstrained (In,Ga)N-GaN SCQW and the corresponding confinement potential.

$$V(z)=\begin{cases}0 & \frac{L_b}{2}\le|z|\le\left(L_w+\frac{L_b}{2}\right),\\ V_0=Q_c\Delta E_g^{\Gamma} & \text{elsewhere}\end{cases}\tag{2}$$

Q_c and ΔE_g^{Γ} are, respectively, the conduction band offset and the energy difference between the barrier and the well at Γ-point [14, 15]. In order to obtain the impurity-related eigen-values and the corresponding eigenfunctions, we have used the traditional Ritz variational approach. The trial wave-function is taken as the product of the hydrogenic function $\Gamma_n^l(r)$, of the n-th state and with l symmetry, with the ground-state wave-function $\phi_0(z)$. This latter can be obtained easily by the standard solution of the Hamiltonian without the impurity. For the lowest-excited state and the ground-state hydrogenic functions, we have used the same as those of Refs. [16, 17].

For small incident pump intensity, the analytical expressions of the linear and the third-order nonlinear ACs are given as [18]:

$$\alpha^{(1)}(\omega)=\sqrt{\frac{\mu}{\varepsilon^*\varepsilon_0}}\frac{\tau_{12}\left|M_{21}\right|^2\sigma\omega}{\hbar\left[(\omega_{fi}-\omega)^2\tau_{12}^2+1\right]},\tag{3}$$

$$\alpha^{(3)}(\omega,I)=-\sqrt{\frac{\mu}{\varepsilon^*}}\left(\frac{I}{2\varepsilon_0 n_{\mathrm{r}}c}\right)\frac{4\tau_{21}\left|M_{21}\right|^4\sigma\omega}{\hbar\left[(\omega_{21}-\omega)^2\tau_{21}^2+1\right]}$$

$$\times\left[1-\frac{\rho_{21}}{4\left|M_{21}\right|^2}\frac{3\tau_{21}^2\omega_{21}^2-4\tau_{21}^2\omega\omega_{21}+\left(\tau_{21}^2\omega^2-1\right)}{\tau_{21}^2\omega_{21}^2+1}\right].\tag{4}$$

Notice that n_{r} represents the refractive index of the semiconductor, c is the speed of the light in vacuum, ε_0 is the static electrical permittivity of the vacuum and I $\left(=2\varepsilon_0 n_{\mathrm{r}}c\left|E\right|^2\right)$ is the incident pump intensity. The incident photon angular frequency is ω, μ is the permeability of the system and τ_{21} is the relaxation time. The electron density in the well is given as $\sigma=N/V$ for which N is the number of electrons in the well while V is its volume and so it depends as L_w^{-1}. The difference of the energy between final and initial states is given as $E_{21}=E_2-E_1=\hbar\omega_{21}$. The ρ_{21} is given as $\rho_{21}=\left|M_{22}-M_{11}\right|^2$ while the M_{fi} $(=\langle\psi_f\left|ez\right|\psi_i\rangle)$ is the dipole transition matrix element between i-th (lower) and f-th (upper) states. Therefore, the total ACs can be obtained as the sum of both contributions.

3. Results and discussion

In the present section, our calculations are carried out for typical Wurtzite unstrained $In_xGa_{1-x}N$-GaN SCQW. The parameters used are as follows: $\tau_{21}=0.2$ ps, $n_{\mathrm{r}}=3.4$, $T=300$ K, $I=25$ MW m^{-2}, $x=0.2$ and $\sigma=2\times10^{16}$ cm^{-3}. The width is given in the effective Bohr radius $a^*=\varepsilon_0\hbar^2/m^*e^2$. In contrast, the linear, nonlinear and total OACs of (In,Ga)N-GaN SCQW and uncoupled symmetric QW (SQW) are plotted in Fig. 2 as a function of the incident photon energy for $L_w=5$ and $L_b=3$. We notice that the amplitude of all OACs is given in term of that of the linear component of SQW. It is clearly observed that the OACs are non-monotonic functions of the photon energy. The OACs reach their maxima at some positions. Compared to SQW, it is easily seen that larger OACs are obtained in the SCQW. This is in good agreement with the results of Refs. [6, 12, 13]. It can be also seen that the nonlinear term is more enhanced in the SCQW and then, it should be taken into account of its contribution especially for the experimental studies.

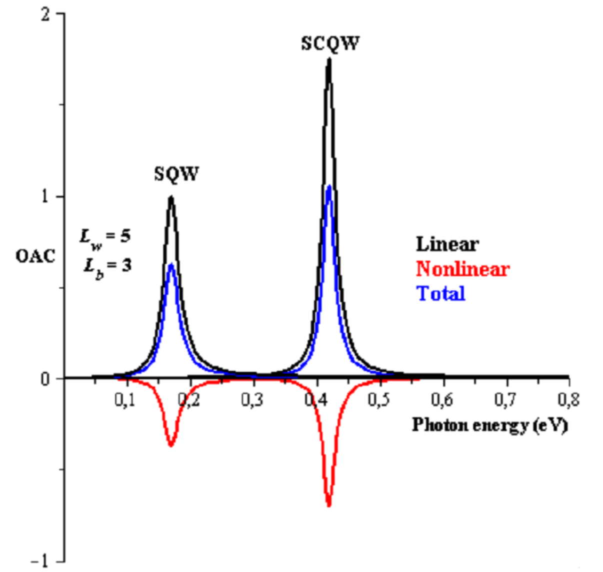

Fig. 2. Linear, nonlinear and total OACs of unstrained $In_{0.2}Ga_{0.8}N$-GaN-SCQW and SQW as a function of the photon energy at room temperature.

In Fig. 3, we present the results corresponding to OACs versus the photon energy for three values of the well widths: $L_w=3$, 5 and 7 and for $L_b=2$. It is shown that the well width has a great impact on the optical properties as expected. The main feature of this figure is that the resonant peaks of all OACs move lower energies, red-shift, as L_w increases. This is due to the fact that as L_w increases, the quantum confinement effect becomes weaker and then the energy difference be-

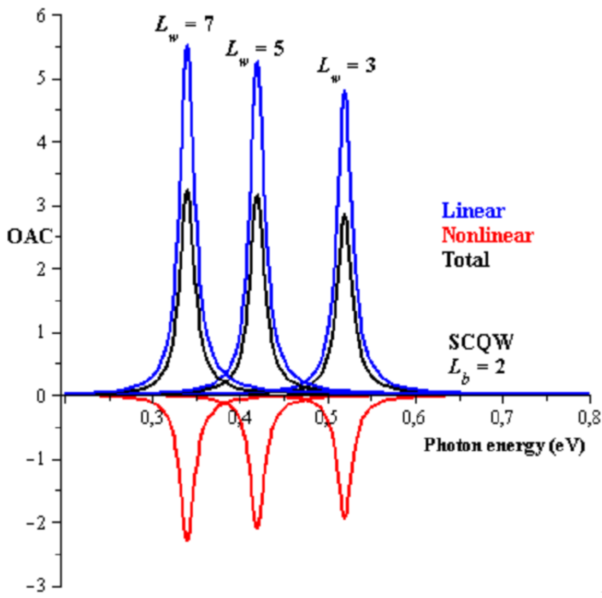

Fig. 3. Linear, nonlinear and total OACs of unstrained $In_{0.2}Ga_{0.8}N$-GaN-SCQW as a function of the photon energy for $L_b = 2$ at room temperature. The effect of the well width is included.

tween the implied states decreases for finally to tend to the continuum bulk limit. Additionally, it appears that the amplitudes of the OACs are enhanced when L_w increases. The physical reason is that the dipole transition matrix element increases versus L_w due to a large overlap between the electronic wave functions. On the other hand, with increase of L_w the electron density decreases. These two parameters act in the opposite sense but our results exhibit that the increase rate of $|M_{21}|^2$ dominates the decrease one of σ.

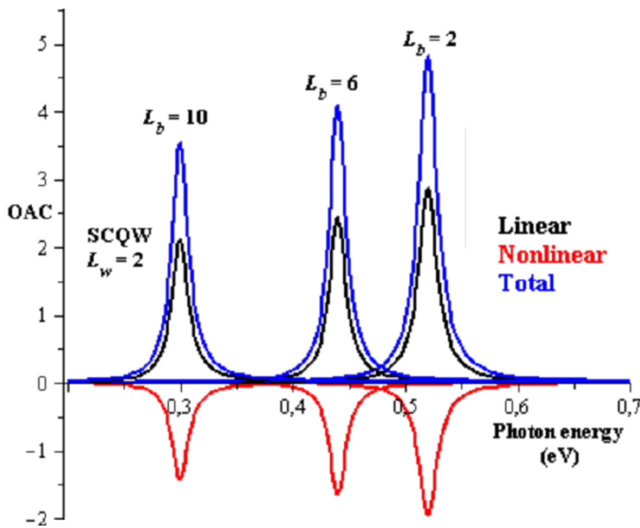

Fig. 4. Linear, nonlinear and total OACs of unstrained $In_{0.2}Ga_{0.8}N$-GaN-SCQW as a function of the photon energy for $L_w = 2$ at room temperature. The effect of the barrier width is introduced.

Figure 4 shows the linear, nonlinear and total OACs of (In,Ga)N-GaN unstrained SCQW according to $\hbar\omega$ for three values of the barrier widths: $L_b = 2$, 6 and 10 and for $L_w = 3$. It is shown that the OACs are strongly dependent on barrier width. The amplitudes of OACs decrease also as L_b increases. This is due to the fact that as L_b increases the coupling between the right-well and the left-well diminishes which induces an important decrease of the overlap integral of the wave functions. As a result, a weaker M_{21} will be obtained which ultimately leads to a significant decrease of the OACs amplitude, i.e., the thinner the barrier region is, the greater the amplitude of OACs will be. In the same time, with increase of the barrier width an important displacement of all OACs resonant peaks to lower energies, red-shift, is obtained. This behavior can be attributed to the fact: as L_b increases the repulsion between the wave functions in both wells decreases and then the energy difference between the implied states diminishes. Therefore, the resonant peaks of the OACs red-shift with increase of L_b. It is interesting to mention that in the limit of a large L_b, the optical properties of SCQW converge to those of uncoupled double QW.

Finally, it is interesting to mention that the results presented above are in good agreement with those reported in the literature concerning symmetric and asymmetric coupled quantum system based on different semiconductor materials [8–13].

4. Conclusion

In this work, linear, third-order nonlinear and total OACs associated with intra-conduction band transition in unstrained symmetric $In_0.2Ga_0.8N$-GaN coupled QWs are computed. The effect of the structure size is investigated within the framework of the single band effective-mass and one parabolic band approximations. Our results depict that:

- The coupling enhances the OACs.
- An important red-shift is obtained as the well and/or the barrier width increase.
- The amplitude of the OACs increases (decreases) versus the well (barrier)-width.

Due to the importance of (In,Ga)N semiconductor material, we hope that this theoretical investigation may have consequences about practical application of electro-optical devices and optical communication and will be useful for further understanding the considerable effects of the coupling on the optical properties.

References

[1] E. Rosencher, P. Bois, *Phys. Rev. B* **44**, 11315 (1991).

[2] L. Zhang, H.J. Xie, *Phys. Rev. B* **68**, 235315 (2003).

[3] J.L. Liu, Y.C. Bai, G.G. Xiong, *Physica E* **23**, 70 (2004).

[4] C.G. Zhang, K.X. Guo, *Physica B* **383**, 183 (2006).

[5] Z.E. Lu, K.X. Guo, *Commun. Theor. Phys.* **45**, 171 (2006).

[6] L. Zhang, *Superlatt. Microstruct.* **37**, 261 (2005).

[7] I. Saidi, L. Bouzaine, H. Mejri, H. Maaref, *Mater. Sci. Eng. C* **28**, 831 (2008).

[8] L. Zhang, Y.M. Chi, J.J. Shi, *Phys. Lett. A* **366**, 256 (2007).

[9] M. Bedoya, A.S. Camacho, *Phys. Rev. B* **72**, 155318 (2005).

[10] T.I. Park, G. Gumbs, Y.C. Chen, *J. Appl. Phys.* **86**, 1467 (1999).

[11] E. Ozturk, I. Sokmen, *Superlatt. Microstruct.* **41**, 36 (2007).

[12] H. El Ghazi, A John Peter, *Solid State Comm.* **201**, 5 (2015).

[13] M.J. Karimi, A. Keshavarz, A. Poostforush, *Superlatt. Microstruct.* **49**, 441 (2011).

[14] H. El Ghazi, I. Zorkani, A. Jorio, *Physica B Condens. Matter* **412**, 87 (2013).

[15] H. El Ghazi, A. Jorio, I. Zorkani, *Physica B Condens. Matter* **410**, 49 (2013).

[16] H. Panahi, M. Maleki, *J. Appl. Sci.* **8**, 636 (2008).

[17] H. El Ghazi, A. Jorio, I. Zorkani, *Physica B Condens. Matter* **426**, 155 (2013).

[18] E. Paspalakis, J. Boviatsis, S. Baskoutas, *J. Appl. Phys.* **114**, 153107N (2013).